Proc. Natl. Acad. Sci. USA
Vol. 92, pp. 8358–8362, August 1995
Immunology

Radiometal labeling of recombinant proteins by a genetically engineered minimal chelation site: Technetium-99m coordination by single-chain Fv antibody fusion proteins through a C-terminal cysteinyl peptide

(antibody engineering/immunotargeting/tumor imaging/recombinant radiometal chelate)

ANDREW J. T. GEORGE*††‡, FRANÇOIS JAMAR†§¶, MEI-SHENG TAI‖, BRIDGET T. HEELAN*, GREGORY P. ADAMS**, JOHN E. MCCARTNEY‖, L. L. HOUSTON††, LOUIS M. WEINER**, HERMANN OPPERMANN‖, A. MICHAEL PETERS§, AND JAMES S. HUSTON‡‖

Departments of *Immunology and §Diagnostic Radiology, Royal Postgraduate Medical School, Hammersmith Hospital, Du Cane Road, London W12 0NN, United Kingdom; ‖Creative BioMolecules, Inc., 45 South Street, Hopkinton, MA 01748; **Department of Medical Oncology, Fox Chase Cancer Center, Philadelphia, PA 19111; and ††Prizm Pharmaceuticals, Inc., San Diego, CA 92101

Communicated by Herman N. Eisen, Massachusetts Institute of Technology, Cambridge, MA, April 24, 1995

ABSTRACT **We describe a method to facilitate radioimaging with technetium-99m (^{99m}Tc) by genetic incorporation of a ^{99m}Tc chelation site in recombinant single-chain Fv (sFv) antibody proteins. This method relies on fusion of the sFv C terminus with a Gly_4Cys peptide that specifically coordinates ^{99m}Tc. By using analogues of the 26-10 anti-digoxin sFv as our primary model, we find that addition of the chelate peptide, to form 26-10-1 sFv′, does not alter the antigen-binding affinity of sFv. We have demonstrated nearly quantitative chelation of 0.5–50 mCi of ^{99m}Tc per mg of 26-10-1 sFv′ (1 Ci = 37 GBq). These ^{99m}Tc-labeled sFv′ complexes are highly stable to challenge with saline buffers, plasma, or diethylenetriaminepentaacetic acid. We find that the ^{99m}Tc-labeled 741F8-1 sFv′, specific for the c-erbB-2 tumor-associated antigen, is effective in imaging human ovarian carcinoma in a *scid* mouse tumor xenograft model. This fusion chelate methodology should be applicable to diagnostic imaging with ^{99m}Tc and radioimmunotherapy with ^{186}Re or ^{188}Re, and its use could extend beyond the sFv′ to other engineered antibodies, recombinant proteins, and synthetic peptides.**

Antibody engineering provides an opportunity for the development of diagnostic imaging agents that incorporate superior radiolabeling methodologies in the design of the targeting molecules. As one example of this approach, the present study involves engineering ^{99m}Tc chelation sites into single-chain Fv (sFv) proteins. These are recombinant forms of the minimal antibody combining site, consisting of antibody heavy chain variable and light chain variable domains connected by a peptide linker (1). Due to their small size, sFv proteins have a faster blood clearance, greater tissue penetrance (2), and potentially lower immunogenicity than IgG, $F(ab')_2$, or Fab. The sFv may be assembled from the variable regions of particular monoclonal antibodies (1) or made *de novo* from phage display libraries (3, 4), with high yields possible by using bacterial expression systems (5, 6). Monovalent sFv and their bivalent derivatives, such as $(sFv')_2$ dimers, are particularly well suited to *in vivo* applications (7) and can be used for imaging of neoplastic disease (2, 4, 7) and myocardial infarction (8) and for targeting cytotoxic agents to tumor cells (9, 10).

Technetium-99m (^{99m}Tc) is the preferred radionuclide for clinical imaging, having superior physical properties, ready availability, low cost, and easy disposal. The sFv is a particularly suitable delivery vehicle for ^{99m}Tc, as the rapid clearance of circulating sFv allows high-contrast imaging within the 6-hr half life of ^{99m}Tc (8). We have used chemical conjugates of the RP-1 chelate with sFv to prepare ^{99m}Tc-labeled sFv species (8, 11). However, such methods necessitate specialized expertise in coupling chemistry and typically result in heterogeneous products with possible damage to the labeled protein (12). IgG can be labeled directly with ^{99m}Tc through hinge-region cysteine residues (13), but unmodified sFv cannot be directly labeled, as the conserved cysteine pairs in each variable domain form essential disulfide bonds.

In this paper, we explore radiometal binding and targeting by sFv fusions with cysteinyl peptides, termed sFv′ (7), that allow rapid one-step site-specific labeling of sFv′ with ^{99m}Tc. We show that fusion of this peptide has no deleterious effect on the immunoreactivity or biodistribution of the sFv. Such genetically fused sFv′ chelates could make the preparation of ^{99m}Tc-labeled sFv′ species readily accessible for *in vitro* binding analysis and *in vivo* targeting. These sFv′ chelates also avoid the complications of binding radiometals by a large fusion partner, such as metallothionein (14, 15), which could perturb sFv folding and alter its biodistribution properties.

MATERIALS AND METHODS

Design and Preparation of sFv Proteins. Our primary model was the 26-10 sFv, which recognizes digoxin and related cardiac glycosides such as ouabain (1). For tumor localization studies, we used the 741F8 sFv, which targets the tumor-associated antigen c-erbB-2 (7, 16). The 26-10-1 sFv′ and 741F8-1 sFv′ were fusions with a C-terminal Gly_4Cys peptide; the 26-10-1 sFv′ had a Ser between the light chain variable region and Gly_4Cys. All sFv had a (heavy chain variable region)–linker–(light chain variable region) format, with the linker sequence being either SerGly-$(Ser_4Gly)_2$-Ser for 26-10-1 sFv′ and its 26-10/S sFv control or $(Ser_4Gly)_2$-Ser_4 for 741F8-1 sFv′ (16). These proteins were expressed in *Escherichia coli* as cytoplasmic inclusion bodies, which were refolded and isolated as described (16, 17). The sFv′ species were stored as stable $(sFv')_2$ dimers.

Kinetics of Antigen Binding by sFv Proteins. Kinetic binding studies were performed by using the IAsys resonant mirror biosensor (Fisons Applied Sensor Technology, Cambridge,

The publication costs of this article were defrayed in part by page charge payment. This article must therefore be hereby marked "*advertisement*" in accordance with 18 U.S.C. §1734 solely to indicate this fact.

Abbreviations: BSA, bovine serum albumin; DTPA, diethylenetriaminepentaacetic acid; ITLC, instant thin-layer chromatography; sFv, single-chain Fv; TCA, trichloroacetic acid.

†A.J.T.G. and F.J. contributed equally to this paper.

‡To whom reprint requests should be addressed.

¶Present address: Université Catholique de Louvain, Centre de Médecine Nucléaire, Brussels, Belgium.

U.K.) (18). Ouabain–bovine serum albumin (BSA) [50 μg/ml in 10 mM sodium acetate (pH 4.5)], prepared as noted for digoxin–BSA (17), was coupled to the sensing surface of the cuvette (18). Duplicate samples of 26-10/S sFv and reduced 26-10-1 sFv′, at six concentrations from 23 nM to 740 nM, were added to the cuvette and the association reaction was monitored for 5 min. The surface was washed four times in Dulbecco's phosphate-buffered saline (PBS), pH 7.3/0.05% Tween 20, and the dissociation reaction was followed for 5 min. The biosensor surface was regenerated by washing for 2 min in 50 mM HCl. Analysis of data with the FASTFIT program yielded rate constants for association (k_a) and dissociation (k_d) (18).

Standard Radiolabeling Conditions. The 26-10-1 sFv′ and 741F8-1 sFv′ were reduced for 2 hr at pH 7.3 with 2-mercaptoethanol (1000-fold molar excess over sFv′) to give sFv′ with a free sulfhydryl suitable for ^{99m}Tc incorporation. The proteins were separated from the reducing agent on a PD-10 gel column (Pharmacia) equilibrated in PBS at pH 7.3 (N_2 purged) or on a Sephadex G-50-80 spin column. The sFv′ proteins were used immediately or some 26-10-1 sFv′ was stored at −70°C in PBS before use, which leaves binding properties unaltered. The [^{99m}Tc]pertechnetate ($^{99m}TcO_4^-$) was obtained by elution of a ^{99}Mo/^{99m}Tc generator (Amertech II, Amersham and Mallinckrodt) with saline (0.15 M NaCl) at pH 7. It was used within 4 hr of elution and diluted with an equal volume of 0.2 M Tris·HCl/0.2 M arginine, pH 10, to give a final activity of 185 MBq/ml (5 mCi/ml). Stannous fluoride was used as reducing agent; for convenience, we used a commercial kit containing 5 mg of medronate (methylene diphosphonate), 0.34 mg of SnF_2, and 2 mg of sodium *p*-aminobenzoate (Amerscan Medronate II Agent; Amersham, U.K., or Medi-Physics, Woburn, MA) diluted in 2.0 ml of saline immediately before use. Each reaction vial comes purged with nitrogen; saline is added by injection through a gas-tight septum, preventing oxidation of the stannous fluoride. Labeling was done in a 1.5-ml microcentrifuge tube in which 50 μg of the sFv′ (in 100 μl of PBS) was mixed with 8.5 μg of SnF_2 (50 μl of Medronate II preparation), and then 100 μl of $^{99m}TcO_4^-$ was added (18.5 MBq). The mixture was incubated at room temperature for 60 min. The labeling efficiency was determined by instant thin-layer chromatography (ITLC) using 1 × 10 cm ITLC-SG strips (Gelman) with PBS as the mobile phase, to measure the sFv′-bound ^{99m}Tc (13); the presence of ^{99m}Tc colloid was also monitored (19).

Optimization of the Labeling Conditions. Experiments were conducted to determine the optimal labeling conditions for the 26-10-1 sFv′. The pH of the reaction was varied by altering the pH of the $^{99m}TcO_4^-$ solution between 7.5 and 12.0 by addition of 0.2 M Tris/0.2 M arginine (pH 10 or 12) and 0.1 M citric acid (pH 3.0). Different incubation times were used, from 30 sec to 120 min. The amount of radioactivity used was increased from 185 to 18,500 MBq/mg of sFv′ (5–500 mCi). In all experiments, the reaction volume was kept as close as possible to 250 μl.

Stability Studies of sFv′ Radiometal Complexes. The stability of the ^{99m}Tc binding to 26-10-1 sFv′ samples was measured 24 hr after storage or incubation in 40 vol of saline, PBS, fresh human plasma, or diethylenetriaminepentaacetic acid (DTPA), at a DTPA/sFv ratio of 1000:1 (final volume, 250 μl). The percentage of ^{99m}Tc remaining bound after 24 hr was determined by using ITLC (saline and PBS) or precipitation with 5% (wt/vol) trichloroacetic acid (TCA) for 10 min (plasma).

Radioiodination of the 26-10-1 sFv′. The 26-10-1 sFv′ was iodinated as described by Salacinski *et al.* (20). The specific activity of the radiolabeled antibody was 70 MBq/mg (1.9 mCi/mg) and, by TCA precipitation, 98.9% of the radioactivity was protein bound. In some experiments, the ^{125}I-labeled 26-10-1 sFv′ was further reduced, as above, and alkylated with 150 mM iodoacetamide (16).

Analysis of Radiolabeled Proteins. SDS/PAGE on 12.5% gels assessed reduced or nonreduced samples (21); ^{99m}Tc-labeled sFv′ lanes were imaged by using a γ camera (Starcam AC/T 400 camera, GE, Holte, Denmark) before staining with Coomassie blue, and radioactivity profiles were corrected for background.

Evaluation of Immunoreactivity. Radiolabeled 26-10-1 sFv′ (2 μg/ml, final concentration) was incubated with 100 μl of ouabain-NH_2-Sepharose resin (1:1 with PBS); samples were gently mixed on a rotator for 60 min at room temperature. After centrifugation at 5000 × *g* for 5 min, the beads were washed with 400 μl of PBS containing 0.1% BSA, and their radioactivity was counted; nonspecific binding was <2%.

Biodistribution Studies. Blood clearance studies were performed in male AS rats weighing 222 ± 8 g. They were injected i.v. with ≈10 MBq of ^{99m}Tc-labeled 26-10-1 sFv′ (10 μg) and 0.2 MBq of ^{125}I-labeled 26-10-1 sFv′ (3 μg) in 0.5 ml of saline. Blood samples were taken 5, 15, 30, 60, 120, 180, and 240 min after injection. For organ distribution analysis, animals were killed by exsanguination at 4 hr or 24 hr after injection of the radiolabeled 26-10-1 sFv′ and tissues were collected. Tissue radioactivity was measured immediately after the experiments for ^{99m}Tc and 5 days later for ^{125}I. The protein-bound radioactivity in plasma was measured at three times by using TCA precipitation, and the immunoreactivity was determined by incubating 50 μl of the plasma (diluted 1:4 in heparinized saline) with 100 μl of ouabain beads, as described above.

Imaging Studies of SK-OV-3 Tumors. Four- to six-week-old male C.B17/lcr-*scid* mice were obtained from the Fox Chase Cancer Laboratory Animal Facility. A human ovarian carcinoma cell line (SK-OV-3, HTB 77; American Type Culture Collection) was implanted s.c. (2.5×10^6 SK-OV-3 cells at logarithmic phase) on the abdomen. Each of the five mice with tumors of 350–600 mg was given 12 MBq (93 μg) of ^{99m}Tc-labeled 741F8-1 sFv′ by tail vein injection. At 1, 6, and 24 hr, mice were anesthetized (7), and 20,000-count images were acquired by using a Prism 2000XP γ camera (Picker, Highland Heights, OH) equipped with a low-energy collimator.

RESULTS AND DISCUSSION

Two distinct sFv′ proteins were utilized in this study, the anti-digoxin 26-10-1 sFv′ for optimization of labeling conditions, and the 741F8-1 sFv′ for tumor imaging of c-erbB-2 which is overexpressed in a significant fraction of breast and ovarian carcinomas. Both sFv′ species have C-terminal Gly_4Cys as a peptide chelate, which was chosen to provide for N_3S coordination of ^{99m}Tc. Mercaptoacetyltriglycine is another such N_3S chelate (22) that is used in renal imaging and is the moiety that coordinates ^{99m}Tc within the RP-1 bifunctional chelate (23). These N_3S chelates typically coordinate ^{99m}Tc as oxotechnetium, forming a square planar complex (22, 24). Thus, the Gly_4Cys peptide is expected to coordinate ^{99m}Tc through its amide nitrogens and the terminal cysteine. The glycines allow maximal flexibility of the peptide to facilitate chelation of ^{99m}Tc without disrupting the structure of adjacent framework regions. For N_3S coordination of ^{99m}Tc, the sFv′ terminal cysteine must be in a reduced state. In the present experiments, the starting material for labeling was $(sFv')_2$, which was gently reduced to form sFv′ species with the requisite free sulfhydryl.

The entire Fv region architecture is intimately involved in maintaining the integrity of the antibody combining site. Small perturbations of variable domain structure can thus produce large changes in binding, as observed for 26-10 sFv, where association with a secondary antibody lowered sFv affinity for digoxin (25). Therefore, the kinetics of 26-10-1 sFv′ binding with ouabain were compared to those of 26-10/S sFv. The two proteins show the same rate and equilibrium constants within experimental error (Table 1), indicating that fusion of the chelation peptide within the 26-10-1 sFv′ had no deleterious effect on binding of ouabain.

Table 1. Kinetic analysis of 26-10/S sFv and 26-10-1 sFv′ binding to ouabain–BSA

Sample	k_a, $M^{-1}\cdot sec^{-1}$	k_d, sec^{-1}	K_d, M
26-10/S sFv	$(4.5 \pm 0.3) \times 10^4$	$(9.7 \pm 1.4) \times 10^{-3}$	$(2.1 \pm 0.3) \times 10^{-7}$
26-10-1 sFv′	$(4.9 \pm 0.3) \times 10^4$	$(11.4 \pm 2.3) \times 10^{-3}$	$(2.3 \pm 0.5) \times 10^{-7}$

Labeling of sFv′ with ^{99m}Tc. Initial experiments showed that mildly reduced monomeric 26-10-1 sFv′ could be efficiently labeled with ^{99m}Tc, whereas very poor labeling of unreduced 26-10-1 $(sFv')_2$ was achieved. Furthermore, no significant labeling was observed if the chelate peptide was absent, as the 26-10/S sFv exhibited only 6.4 ± 2.7% incorporation of ^{99m}Tc. This substantiates that the reduced C-terminal peptide is the primary chelation site for ^{99m}Tc in the sFv′. A standard labeling protocol was devised: a 50-μg sample of reduced 26-10-1 sFv′ (0.5 mg/ml) was combined with 18.5 MBq of [^{99m}Tc]pertechnetate at pH 10, in the presence of 0.22 mM stannous fluoride (final pH of reaction, ≥9.5). This consistently resulted in a labeling efficiency >97% after a 60-min incubation, with little formation of colloidal species (<2%, n = 5). This high efficiency ensures that the radiolabeled material needs no further purification for clinical purposes.

The pH of the $^{99m}TcO_4^-$ was varied to find the optimal pH for the labeling reaction. Efficient labeling was only seen when the alkaline pH of the $^{99m}TcO_4^-$ resulted in a final pH of at least 9.5 (Fig. 1*A*). While the relatively high pH optimum of the reaction is likely to be acceptable for many sFv proteins, suboptimal labeling under less basic conditions may be used for more sensitive proteins. Scaled-up experiments demonstrated that as much as 1850 MBq (50 mCi) could be added to 1 mg of sFv′ while maintaining a labeling efficiency >97% (Fig. 1*B*). Conditions that minimize oxidation of the sFv′ to $(sFv')_2$ dimers, prior to chelation of ^{99m}Tc, could potentially increase this upper limit of specific activity. A time course of the labeling reaction demonstrated that most of the labeling occurred within 30 min (Fig. 1*C*).

The presence of stannous ions to reduce the $^{99m}TcO_4^-$ was essential for successful labeling of the sFv′. The kit used in these studies (Medronate II) is not readily available in the United States, where the corresponding kit (MDP Multidose, Amersham) has a somewhat different composition that required different conditions for optimal labeling (data not shown). Other commercial kits containing Sn^{2+} can presumably be used after appropriate optimization.

Covalent and Noncovalent Dimerization of the Radiolabeled sFv′ Proteins. SDS/PAGE analysis, under nonreducing conditions, was performed on the ^{99m}Tc-labeled 26-10-1 sFv′. Although some of the sFv′ had oxidized to disulfide-linked $(sFv')_2$ dimer (≈55 kDa), possibly prior to labeling, virtually all the ^{99m}Tc activity was associated with the monomeric form (Fig. 2). Similar results were obtained with the 741F8-1 sFv′. This suggests that once ^{99m}Tc and the terminal cysteine have formed a coordination complex, neither is able to mediate formation of ^{99m}Tc-labeled $(sFv')_2$ covalent dimer. When the sFv′ was radioiodinated as described Salacinski *et al.* (20), the ^{125}I activity was associated with both the monomeric and dimeric forms.

Size-exclusion chromatography under native conditions showed that the ^{99m}Tc- and ^{125}I-labeled 26-10-1 sFv′ species were present as both monomeric and dimeric forms of the sFv′ (data not shown). This was observed for ^{125}I-labeled 26-10-1 sFv′, even when the molecule was reduced and alkylated, in agreement with previous observations indicating that 26-10-1 sFv′ self-associates to form a mixture of monomers and noncovalent dimers in solution (16).

Stability and Immunoreactivity of Radiolabeled 26-10-1 sFv′ *in Vitro* and *in Vivo*. The ^{99m}Tc-labeled 26-10-1 sFv′ demonstrated excellent stability, since no significant amount of free [^{99m}Tc]pertechnetate was generated after 24-hr incubations in saline, PBS (pH 7.3), or fresh human plasma (Table 2). Transchelation challenge with a 1000:1 molar ratio of DTPA/sFv′ for 24 hr did not result in any significant displacement of the ^{99m}Tc from the sFv′. After radiolabeling with ^{99m}Tc, the 26-10-1 sFv′ retained most of its immunoreactivity with 74.2 ± 3.9% (n = 8) of the radiolabeled material binding to ouabain beads. The immunoreactivity observed after ^{125}I labeling was less (53.8 ± 6.6%, n = 4), suggesting that this method can damage the antigen binding site.

The *in vivo* stability and immunoreactivity of radiolabeled sFv′ were analyzed after injection in rats of ^{99m}Tc- and ^{125}I-labeled 26-10-1 sFv′. TCA precipitation of plasma, obtained as a function of time after administration of radiolabeled sFv′, showed the protein-bound radioactivity was higher for the ^{99m}Tc-labeled 26-10-1′ sFv′ than for the ^{125}I-labeled control (expressed as

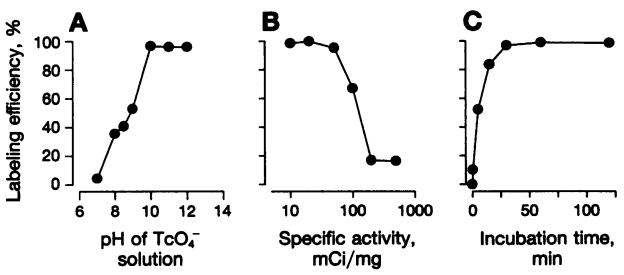

FIG. 1. Optimization of labeling conditions. The ^{99m}Tc labeling of the 26-10-1 sFv′ was carried out under a variety of conditions, and the labeling efficiency was determined by ITLC. The pH optimum of the labeling experiment was determined in *A* by varying the pH of the [^{99m}Tc]pertechnetate solution as eluted from the generator. In *B* and *C*, the labeling was performed by using a standard protocol at pH 10 in *B* varying the amount of $^{99m}TcO_4^-$ added or in *C* varying the duration of the reaction.

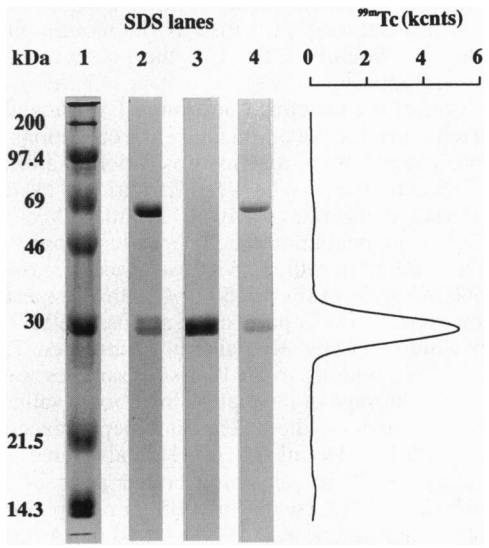

FIG. 2. SDS/PAGE characterization of the unlabeled and ^{99m}Tc-labeled 26-10-1 sFv′ species. All samples were electrophoresed on a SDS/12.5% polyacrylamide gel. Lanes: 1, molecular weight markers; 2, unreduced 26-10-1 sFv′ showing a majority of dimeric material at 55 kDa; 3, same as lane 2 in reducing conditions; 4, ^{99m}Tc-labeled 26-10-1 sFv′ (nonreducing conditions). This photograph is a composite taken from the same gel. To the right is a radiochromatogram of lane 4 generated from a 30-min γ camera image; ^{99m}Tc levels are shown in thousands of counts accumulated (Kcnts).

percentage of the initial value for each species): 88.1 ± 5.7% vs. 71.7 ± 6.2% (not significant) at 60 min and 56.5 ± 1.9% vs. 37.4 ± 11.5% ($P < 0.05$) at 240 min. Also, while at 5 min neither species had lost any immunoreactivity, at 240 min the ^{99m}Tc-labeled material retained 82.6 ± 6.4% of its original immunoreactivity and the ^{125}I species had only 40.6 ± 6.8% ($P < 0.005$).

Pharmacokinetics. In biodistribution studies using simultaneous injection of the ^{99m}Tc- and ^{125}I-labeled 26-10-1 sFv′ in rats, both species displayed biexponential time–activity curves with a rapid equilibration phase (half-life = $t_{½\alpha}$) and subsequent elimination phase (half-life = $t_{½\beta}$). The blood clearance of the ^{99m}Tc-labeled sFv′ was faster than that of the ^{125}I-labeled sFv′ (Fig. 3) with $t_{½\alpha}$ values of 8.3 ± 1.6 min and 6.4 ± 1.2 min (not significant) and $t_{½\beta}$ values of 81.4 ± 10.6 min and 153.3 ± 26.6 min ($P < 0.01$) for ^{99m}Tc-labeled 26-10-1 sFv′ and ^{125}I-labeled 26-10-1 sFv′, respectively. It is noteworthy that at 4 hr <5% of the original ^{99m}Tc activity was found in the circulation, emphasizing that rapidly clearing sFv is an appropriate vehicle for the delivery of short-lived isotopes such as ^{99m}Tc.

The distinct clearance rates of ^{99m}Tc- and ^{125}I-labeled 26-10-1 sFv′ are not due to differences in the size of the radiolabeled protein, as gel chromatography indicated that the two species have similar size distributions (see above). The rapid clearance of the ^{99m}Tc-labeled 26-10-1 sFv′ may be associated with the oxotechnetium-glycine structure expected to form part of the sFv′ coordination complex with ^{99m}Tc, as found in the renal function imaging agent ^{99m}Tc-labeled L,L-ethylenedicysteine (26, 27). It has been speculated that this structure acts in an analogous manner to the carbonyl-glycine motif of agents such as mercaptoacetyltriglycine that bind to renal tubular transport proteins and so are rapidly secreted through the kidneys and into the urine (26, 27). This may be an important feature of the sFv′ protein, as rapid clearance of ^{99m}Tc from the kidney will reduce the radiation dose to that organ.

The organ distributions of the ^{99m}Tc- and ^{125}I-labeled 26-10-1 sFv′ are shown in Table 3. As expected from the rapid clearance of the molecule, after 4 hr ≈13% of the ^{99m}Tc-labeled sFv′ was found in the kidneys, with ≈30% in the urine. By 24 hr, the majority of ^{99m}Tc had cleared through the kidneys, with 1.8% of the radiolabel in the kidneys and 60% in the urine. This contrasts with the results on ^{177}Lu complexed by CC49 sFv through a chemically conjugated chelate, where radioactive material was significantly retained in the kidneys for >6 days (12). Relatively little ^{125}I is associated with the kidneys, due to efficient renal dehalogenation of proteins (12); however, the absolute amount of activity excreted in the urine and feces over 24 hr was similar for both tracers. There was significantly higher ^{99m}Tc activity in the spleen and liver at both 4 and 24 hr, compared to ^{125}I levels. Aside from these three organs, all other tissues exhibited a higher level of ^{125}I-labeled sFv′ than ^{99m}Tc-labeled sFv′, which was probably related to the slower blood clearance of the radioiodinated species. In contrast to the ^{125}I-labeled sFv′, no accumulation of ^{99m}Tc was noted in the stomach and thyroid.

Table 2. Stability of the ^{99m}Tc-labeled 26-10-1 sFv′ complex

Sample	% total radioactivity complexed with sFv′	
	ITLC	TCA precipitation
Control (60 min)	97.6 ± 0.7	92.2 ± 2.0
Control (24 hr)	98.2 ± 2.1	ND
DTPA	97.0 ± 3.6	ND
PBS	96.4 ± 3.6	ND
Saline	97.1 ± 0.5	ND
Serum	ND	92.9 ± 4.8

^{99m}Tc-labeled 26-10-1 sFv′ was prepared and incubated for 24 hr without dilution or after dilution in DTPA, PBS, saline, or serum. The radiopharmaceutical purity of the ^{99m}Tc-labeled sFv′ was then determined, by using ITLC or TCA precipitation, as indicated. In each case, the fraction of total counts that remain complexed by the sFv′ is expressed as the percentage (mean ± SD) from three or more experiments. ND, not done.

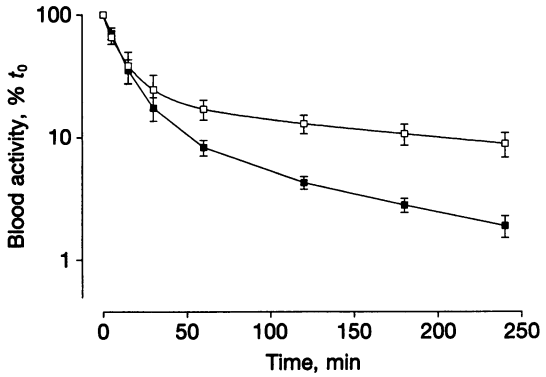

FIG. 3. Clearance of ^{99m}Tc- and ^{125}I-labeled 26-10-1 sFv′ from the circulation. Typical time–activity curves in whole blood of the ^{99m}Tc-labeled 26-10-1 sFv′ (solid squares) and ^{125}I-labeled 26-10-1 sFv′ (open squares) after intravenous injection in rats. Symbols indicate the percentage of the zero time value (mean ± SD) from four animals. The blood clearance of the ^{99m}Tc-labeled sFv′ is clearly faster than that of the ^{125}I-labeled sFv′.

Tumor Localization. Anterior γ camera images were acquired in SK-OV-3 tumor-bearing *scid* mice 1, 6, and 24 hr after intravenous administration of ^{99m}Tc-labeled anti-c-erbB-2 741F8-1 sFv′. Representative images are presented from one mouse (Fig. 4). The images obtained 1 and 6 hr after injection reveal significant accumulation of the ^{99m}Tc-labeled 741F8-1 sFv′ in the tumor, with a variable amount of activity detected in the bladder and significantly less visible in the kidneys. After 24 hr, the tumor was still clearly imaged. Detectable amounts of activity remained in the kidneys, though significantly less was present in the bladder, allowing the observation of some ^{99m}Tc in the bowels. These images compare favorably to those we produced at 24 hr by using ^{131}I-labeled 741F8 sFv in a previous study (7). The ability to clearly image tumor xenografts in the *scid* mouse model as

Table 3. Biodistribution of the ^{99m}Tc- and ^{125}I-labeled 26-10-1 sFv′ in rats

Tissue	% injected dose per g of organ			
	^{99m}Tc-labeled 26-10-1 sFv′		^{125}I-labeled 26-10-1 sFv′	
	4 hr	24 hr	4 hr	24 hr
Blood	0.063	0.012	0.485[b]	0.063[b]
Muscle	0.022	0.002	0.121[b]	0.012[b]
Lung	0.102	0.021	0.427[b]	0.060[a]
Heart	0.030	0.006	0.157[b]	0.020[b]
Thyroid†	0.215*	0.000	314.9[a]*	167.0[a]*
Liver	0.639	0.331	0.273[b]	0.042[b]
Spleen	1.422	0.563	0.339[b]	0.075[b]
Ileum	0.193*	0.025	0.251[NS]	0.080[a]
Colon	0.058*	0.292*	0.166[b]	0.086[NS]*
Stomach	0.118*	0.017	5.055[b]	0.316[b]
Kidney	10.935	1.851	0.768[b]	0.187[b]

Biodistribution of ^{99m}Tc- and ^{125}I-labeled 26-10-1 sFv′ was studied in rats 4 hr ($n = 19$) or 24 hr ($n = 11$) after injection of the radiolabeled antibodies into the animals. The results are expressed as the mean. a, $P < 0.01$; b, $P < 0.001$ between ^{99m}Tc and ^{125}I (paired t test); NS, not significant.

*SEM > 20% of the mean.

†For thyroid, $n = 16$ at 4 hr and $n = 6$ at 24 hr.

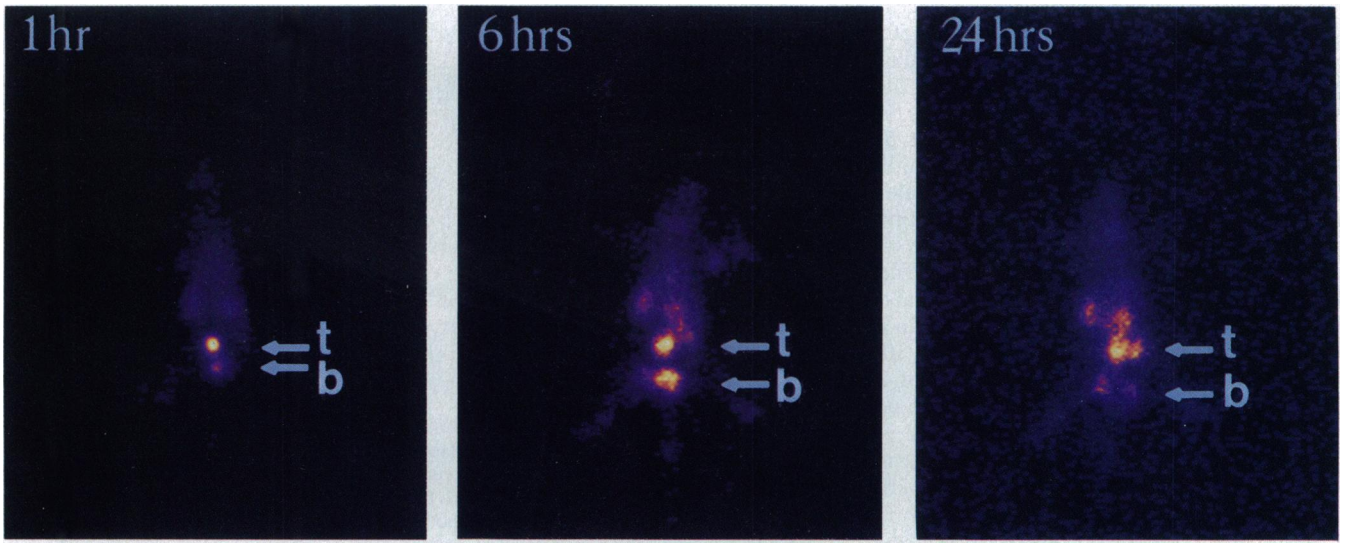

FIG. 4. Imaging of human ovarian tumor xenografts in *scid* mice by ^{99m}Tc-labeled 741F8-1 anti-c-erbB-2 sFv′. γ camera images were obtained 1, 6, and 24 hr after the i.v. administration of ^{99m}Tc-labeled 741F8-1 sFv′ to *scid* mice bearing SK-OV-3 tumor xenografts. The 20,000-count anterior images from a representative mouse with a 478-mg tumor show radioactivity mainly in the tumor (t) and bladder (b). Kidneys are visible as two patches above the tumor. The moderate bladder and kidney activities detectable at 1 and 6 hr were aided by stimulation of urinary output, which would likewise be affected in a clinical setting. The 24-hr image also shows higher relative activity in the kidneys and bowel; in this imaging experiment, the animal was not perfectly flat on the stage, as in the other images, resulting in the asymmetric tumor image. Colors indicate high to low levels of γ emission, ranging from yellow, through orange, to purple for the lowest values.

early as 1 and 6 hr after injection underscores the potential of ^{99m}Tc-labeled sFv′ molecules for tumor imaging.

Conclusion. We have fused the genes coding for sFv proteins with a sequence that encodes a short chelate peptide, Gly_4Cys. Such a fusion protein is readily constructed and combines the minimal antigen binding site with an engineered radiometal coordination site that allows rapid labeling with very high efficiency. The complex formed between the peptide and ^{99m}Tc is stable, *in vitro* and *in vivo*, and can be used to image tumor very effectively. The same approach may also be used to label sFv′ with ^{94m}Tc for positron emission tomography or with ^{186}Re and ^{188}Re for radioimmunotherapy. This strategy should facilitate the development of imaging agents, for basic research and clinical application, and may be extended to other recombinant proteins or synthetic peptides.

This research has been supported by the following: National Cooperative Drug Discovery Group Award U01 CA51880 from the National Cancer Institute, Cancer Research Campaign, the Wellcome Trust, an appropriation from the Commonwealth of Pennsylvania, the Bernard A. and Rebecca S. Bernard Foundation, and the Sir Jules Thorn Charitable Trust. F.J. is supported by the Foundation St. Luc, Brussels.

1. Huston, J. S., Levinson, D., Mudgett-Hunter, M., Tai, M.-S., Novotny, J., Margolies, M. J., Ridge, R. J., Bruccoleri, R. E., Haber, E., Crea, R. & Oppermann, H. (1988) *Proc. Natl. Acad. Sci. USA* **85,** 5879–5883.
2. Yokota, T., Milenic, D. E., Whitlow, M. & Schlom, J. (1992) *Cancer Res.* **52,** 3402–3408.
3. Clackson, T., Hoogenboom, H. R., Griffiths, A. D. & Winter, G. (1991) *Nature (London)* **352,** 624–628.
4. Chester, K. A., Begent, R. H. J., Robson, L., Keep, P., Pedley, R. B., Boden, J. A., Boxer, G., Green, A., Winter, G., Cochet, O. & Hawkins, R. E. (1994) *Lancet* **343,** 455–456.
5. Huston, J. S., George, A. J. T., Tai, M.-S., McCartney, J. E., Jin, D., Segal, D. M., Keck, P. & Opperman, H. (1995) in *Antibody Engineering*, ed. Borrebaeck, C. (Oxford Univ. Press, Oxford), 2nd Ed., pp. 185–227.
6. Ge, L., Knappik, A., Pack, P., Freund, C.& Plückthun, A. (1995) in *Antibody Engineering*, ed. Borrebaeck, C. (Oxford Univ. Press, Oxford), 2nd Ed., pp. 229–266.
7. Adams, G. P., McCartney, J. E., Tai, M. S., Oppermann, H., Huston, J. S., Stafford, W. F., III, Bookman, M. A., Fand, I., Houston, L. L. & Weiner, L. M. (1993) *Cancer Res.* **53,** 4026–4034.
8. Nedelman, M. A., Shealy, D. J., Boutin, R., Brunt, E., Seasholtz, J. I., Allen, I. E., McCartney, J. E., Warren, F. D., Oppermann, H., Pang, R. H. L., Berger, H. J. & Weisman, H. F. (1993) *J. Nucl. Med.* **34,** 234–241.
9. Chaudhary, V. K., Queen, C., Junghans, R. P., Waldmann, T. A., FitzGerald, D. J. & Pastan, I. (1989) *Nature (London)* **339,** 394–397.
10. George, A. J. T., Titus, J. A., Jost, C. R., Kurucz, I., Perez, P., Andrew, S. M., Nicholls, P. J., Huston, J. S. & Segal, D. M. (1994) *J. Immunol.* **152,** 1802–1811.
11. Shealy, D., Nedelman, M., Tai, M.-S., Huston, J. S., Berger, H., Lister-James, J. & Dean, R. T. (1990) *J. Nucl. Med.* **31,** 776–777.
12. Schott, M. E., Milenic, D. E., Yokota, T., Whitlow, M., Wood, J. F., Fordyce, W. A., Cheng, R. C. & Schlom, J. (1992) *Cancer Res.* **52,** 6413–6417.
13. Mather, S. J. & Ellison, D. (1990) *J. Nucl. Med.* **31,** 692–697.
14. Das, C., Kulkarni, P. V., Constantinescu, A., Antich, P., Blattner, F. R. & Tucker, P. W. (1992) *Proc. Natl. Acad. Sci. USA* **89,** 9749–9753.
15. Sawyer, J. R., Tucker, P. W. & Blattner, F. R. (1992) *Proc. Natl. Acad. Sci. USA* **89,** 9754–9758.
16. McCartney, J. E., Tai, M.-S., Hudziak, R. M., Adams, G. P., Weiner, L. M., Jin, D., Stafford, W. F., III, Liu, S., Bookman, M. A., Laminet, A. A., Fand, I., Houston, L. L., Oppermann, H. & Huston, J. S. (1995) *Protein Eng.* **8,** 301–314.
17. Tai, M. S., Mudgett-Hunter, M., Levinson, D., Wu, G. M., Haber, E., Oppermann, H. & Huston, J. S. (1990) *Biochemistry* **29,** 8024–8030.
18. George, A. J. T., French, R. R. & Glennie, M. J. (1995) *J. Immunol. Methods* **183,** 51–63.
19. Thrall, J. H., Freitas, J. E., Swanson, D., Rogers, W. L., Clare, J. M., Brown, M. L. & Pitt, B. (1978) *J. Nucl. Med.* **19,** 796–803.
20. Salacinski, P. R., McLean, C., Sykes, J. E., Clement-Jones, V. V. & Lowry, P. J. (1981) *Anal. Biochem.* **117,** 136–146.
21. Laemmli, U. K. (1970) *Nature (London)* **227,** 680–685.
22. Fritzberg, A. R., Kasina, S., Eshima, D. & Johnson, D. L. (1986) *J. Nucl. Med.* **27,** 111–116.
23. Weber, R. W., Boutin, R. H., Nedelman, M. A., Lister-James, J. & Dean, R. T. (1990) *Bioconjug. Chem.* **1,** 431–437.
24. Saha, G. B. (1992) *Fundamentals of Nuclear Pharmacy* (Springer, New York), 3rd Ed., pp. 98–142.
25. Huston, J. S., Mudgett-Hunter, M., Tai, M. S., McCartney, J., Warren, F., Haber, E. & Oppermann, H. (1991) *Methods Enzymol.* **203,** 46–88.
26. Verbruggen, A. M., Nosco, D. L., Van Nerom, C. G., Bormans, G. M., Adriaens, P. J. & De-Roo, M. J. (1992) *J. Nucl. Med.* **33,** 551–557.
27. Stoffel, M., Jamar, F., Van Nerom, C., Verbruggen, A., Mourad, M., Leners, N., Squifflet, J.-P. & Beckers, C. (1994) *J. Nucl. Med.* **35,** 1951–1958.